

NUMERICAL AND EXPERIMENTAL INVESTIGATIONS OF A HIGH-LOADED TYPICAL MIDDLE STAGE MODEL OF HPC

V.I. Mileshin, I.K. Orekhov, S.V. Pankov, Eu.I Stepanov
Central Institute of Aviation Motors (CIAM)
2, Aviamotornaya St., 111116, Moscow, RUSSIA
E-mail: mileshin@ciam.ru

Keywords: *compressor, blades, aerodynamics, efficiency, loading*

Abstract

Efforts aiming at improvement of compressor efficiency and an increase in stall margin and total pressure ratio using less number of HPC stages in advanced turbofans entail an increase in compressor stage aerodynamic loading. Numerical and experimental investigations of a high-loaded typical HPC middle stage model with respect to effects of longitudinal bending of rotor blades and stator vanes on stage performances are presented in this work. Several versions of the compressor stage are studied. A noticeable increase in adiabatic efficiency is experimentally found for the optimum stage version with "sickle-like" rotor blades. In this version stagger axes of rotor profiles are bent in the circumferential direction in such a way that pressure sides are concave. Moreover, airflow and total pressure ratio are higher. Calculations of stationary viscous flow and parameters of the stage with straight blades are in good agreement with the experiment, but to the present time calculations can't give evidences of a considerable improvement of parameters for the optimum version of the experimental stage.

Nomenclature

G_{cor} – corrected air flow;
 π^* – total pressure ratio;
 η^*_{ad} – adiabatic efficiency;

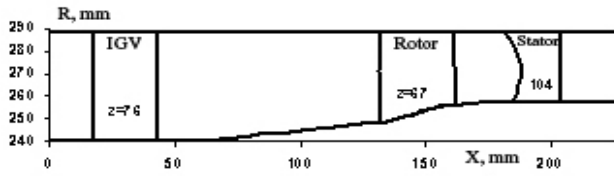
σ – total pressure recovery coefficient;
 λ – flow velocity coefficient relatively to critical sound
 \bar{H}_T – theoretical head coefficient
 Subscripts:
 1 – rotor inlet
 2 – rotor outlet
 3 – before stator
 4 – after stator
 Cor – corrected parameters

Introduction

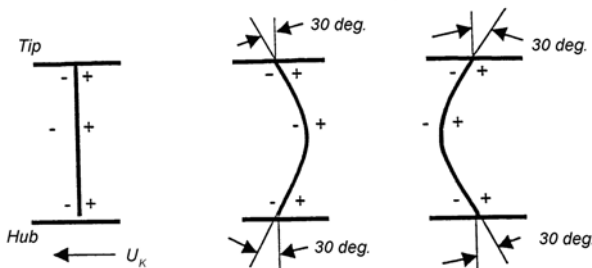
Three-dimensional blades are widely used today in aircraft engine compressors and turbines. Bending and inclinations of supersonic fan rotor blades in axial and circumferential directions are their specific features. Moreover, the blade inclination and bending are not equal in different sections along the blade height. This blade shape is a result of flow optimization aiming at wave loss decrease and reduction of secondary flows intensity as well as blade profile optimization to provide required strength.

An important requirement to compressors of advanced engines is an increase in total pressure ratio but using less number of stages, that results in an increase in aerodynamic loading causing problems in achievement of specified high efficiency and stall margins. For increasing these parameters three guide vane rows of a four-stage high-loaded HPC were bent

and have a scimitar profile. Despite of a small blade height (~14 mm) and medium HPC dimensions, the efficiency reaches $\eta_{ad}^* = 0.87$ at pressure ratio $\pi_k^* > 5$.



Stage flow passage



Straight blade of the initial stage Sabre stator vanes Sickle rotor blades

Fig. 1 Stator vane and rotor blade bending scheme

The objective of this CIAM's research work [2] is to study the effect of blade profile stagger axis bending in the circumferential direction on characteristics of the stage as well as applicability of rotor blades with a bent longitudinal axis for stages with high aerodynamic loading in advanced turbofan compressors. It is considered that bending of the blade longitudinal axis in the circumferential direction changes pressure gradients, modifies flow deceleration along the profiles, aerodynamic loading distribution along the blade row height, losses and lag angles, as well as intensity of secondary flow and flow in docking areas of the blade with the hub and the outer casing.

At the end of 1980s, CIAM completed comparative experimental investigations of stator vanes with curvilinear longitudinal axis without modification of rotor blades. Irrespective of stator vane bending direction, there was an increase in efficiency by 1-2% with simultaneous twice decrease in the periodic component (multiplies to the passing frequency) of total pressure pulsation at the stage outlet [2, 4]. That time it was found that an improvement of stage performances was not a

result of decreased intensity of secondary flows as could be anticipated but, to a great extent, an improvement of rotor performances that was unmodified in comparative tests of the stage with different stators. The test results have not been verified by stationary flow calculations on the basis of various mathematical models. Authors [2, 4] & et al made an assumption that mathematical models for straight and bent blades should take into account a displacement of phase of unsteady interaction of rotor and stator cascades of elementary stages located on different axisymmetrical streamline surfaces along the height.

For more detailed analysis of blade bending effects this work describes numerical-experimental investigations of a high-loaded stage being a prototype of a HPC middle stage for an advanced turbofan.

1 Test object and its instrumentation

The stage has a constant outer diameter - $D_{rotor} = 576$ mm and the following design parameters: $H_T = 0.404$; $C_{1a} = 0.516$; $G_{air.cor} = 11.8$ g/s; $\eta_{ad}^* = 0.88$; $\pi_{stage}^* = 1.52$; $U_{tip.cor} = 327$ m/s.

The stage consists of three blade rows: IGV, rotor and stator. The IGV provides required flow swirling ($\alpha_1 = 65^\circ$) and is located at a proper distance to prevent the influence of its wakes on rotor parameters as well as for instrumentation mounting. The distance between IGV and rotor axes is 115 mm. It is supposed that HPC rotor will have a drum-type design and stator vanes – cantilever-type. To simulate these conditions, the rotor is provided with a part of the drum rotating under the stator vanes.

The stage is designed in such a way that flow inlet and outlet angles are identical and constant along the radius ($\alpha_4 = \alpha_1 = 65^\circ$). There is an increase in the hub diameter within the section from IGV trailing edge to the rotor inlet that results in flow acceleration with an increase in absolute flow velocity angle by 5° . To provide the specified angle at the rotor inlet ($\alpha_1 = 65^\circ$), the flow outlet angle at IGV outlet is taken equal to $\alpha_{out} = 60^\circ$.

The previous research work of high-loaded stages showed that it is advisable to increase the axial velocity component to the outlet. For this reason the flow passage area was decreased from the IGV and behind it, but only in the rotor (due to an increase in the hub diameter); and a cylindrical flow passage is used in the stator ($\bar{d}_1=0.863$, $\bar{d}_2=0.893$, $\bar{d}_4=0.893$).

Rotor blade profiles were found earlier as a result of special research works. They are variable along the blade height; number of rotor blades is $Z_r=67$; blade solidity is $b/t=1.5$ and constant along the radius. Profiles with decreased transverse pressure gradients and lesser losses in the tip clearance are chosen in tip sections. Profiles that are efficient in cascades with increased blade thickness are chosen in hub sections. Standard initial blade profiles are used in middle sections. To prevent blade-casing contact, the tip (mounting) clearance between straight and bent rotor blades was 0.5-0.6 mm – the same as for straight blades.

A decrease in axial velocity component in the tip sections of guide vanes causes a need for an increase of blade solidity. The assumed blade solidity is less than the required value by 25% and is equal to $b/t=1.4$ in the middle radius and $b/t=1.65$ - in tip sections. Number of stator vanes is $Z_{st}=104$. Stator vane chord is $b=23.13$ mm in middle sections and increases up to $b=26.36$ mm at the hub and $b=29.53$ mm at the tip. Superposition of blade profiles is provided along the trailing edge, therefore the leading edge has a variable sweep along the height as shown in Fig. 1 and Fig. 2. To prevent stator vane - drum contact, the tip clearance between the hub and swept vanes is increased up to 0.55-0.70 mm as compared with 0.4-0.5 mm for straight vanes.

The stage was tested at the CIAM's test facility. 1000-KW electric motor was used as a drive of the test facility. Drive power was transmitted via a speed increaser. Torque is measured on the shaft between the speed increaser and the compressor by a torque meter. Power consumption by the compressor shaft friction was estimated on the basis of calibration of running parts in idling for the compressor with a smooth rotor disk.

The stage IGV was an auxiliary row, therefore total pressure losses in IGV were excluded in measurements of the stage performances. Three seven-point pressure rakes were mounted at IGV outlet for measurements of these losses. The IGV casing was movable. Total pressure was measured for 10 positions of the casing with respect to IGV spacing. These rakes were removed in measurements of stage performances, and total pressure losses were calculated on the bases of losses - air flow approximating dependence, $\sigma_{in}(G_{air})$.

Flow parameters at the stage outlet were measured by 6 seven-point pressure rakes and 3 seven-point thermocouples. The rakes were fixed in the rotating ring. Parameters were measured in 5 positions with respect to IGV spacing. An additional five-point total pressure rake was mounted at the rotor outlet. Static pressure on flow passage walls was measured at three points along the circle in inter-blade sections and at the stage outlet.

Four stage configurations produced by combining 2 rotor blade versions and 2 stator vane versions are studied. Rotor blades and stator vanes in the initial stage version are straight. Rotor blades in the 2nd version are sickle-like (Fig.2) and stator vanes – sabre-like, i.e. stagger axes are bent in the circumferential direction in such a way that rotor blade pressure sides and stator vane suction sides are concave.

Among four versions under study the optimum version is chosen that is distinguished by sickle swept rotor blades and straight stator vanes. Tests of the optimum version show a noticeable increase in adiabatic efficiency by $\Delta\eta_{ad}^* \sim 1.7\div 2.0\%$ at $\bar{n}_{cor}=0.8\div 0.9$ of the nominal value and $\Delta\eta_{ad}^* \sim 0.7\%$ at $\bar{n}_{cor}=1.0$. Moreover, there is an increase in airflow and pressure ratio (see Fig. 3). Application of sickle stator vanes is not advisable because of decreased efficiency by $\delta\eta_{ad}^*=1.5\%$ at $\bar{n}_{cor}=0.7-1.0$.

2. Calculations of steady 3D flow and pressure characteristics of the stage and their comparison with experimental data

For the purpose of experimental investigations as well as revealing the grounds of a bending beneficial effect on parameters, a mathematical model was developed and viscous three-dimensional steady flows and integral performances of all stage versions were calculated.

The calculation procedure is based on the numerical solution of 3D Navier-Stokes equations averaged by Reynolds with semi empirical turbulence models and wall functions on the basis of Godunov's implicit high order numerical scheme [1, 3, 5, 6]. Either the Baldwin-Lomacs algebraic turbulence model or differential models can be used for closing the system of equations. The two-parametrical turbulence model $k-\omega$ was used in calculations presented herein for estimation of turbulent viscosity.

Calculations of steady viscous three-dimensional flows were made in «Mixing plane» approximation. Non-stationary interaction of cascades was not taken into account because flow was averaged by a blade-to-blade spacing on the surface separating steady and rotating grid cells. The averaging procedure assumes constancy of momentum flux and energy through this surface. In this case there is an increase in entropy that simulates losses in distortion equalization caused by mixing.

The calculation domain covers three rows and consists of three rectangular (hexagonal) blocks. Each block of the grid covers one blade channel of each row. Calculations are completed for a grid having $(120 \cdot 64 \cdot 64 + 150 \cdot 64 \cdot 64 + 150 \cdot 64 \cdot 64) = 1720320$ cells. In the tip clearance between rotating rotor blades and the fixed outer casing as well as between motionless stator vanes with cantilever attachment and the rotating drum-type hub are 12 cells. The tip clearance values in operating conditions are chosen equal 0.27 mm or 0.76 % of the rotor blade height and 0.15 mm or 0.5 % of the stator vane height. The computational grid in the rotor and in the stator is shown in Fig. 5.

Distributions of total pressure, temperature, an angle between the absolute velocity vector and the meridian plane, and an angle between the velocity vector meridian component and the

stage axis are specified as the boundary conditions at the inlet. Static pressure at the hub is specified at the outlet and pressure distribution along the channel height is derived from the condition of an approximate radial equilibrium. Viscous flow calculations are completed using the standard boundary conditions at the inlet: total temperature = 288.15°K, total pressure = 101325 Pa, flow angles at IGV inlet are equal to zero.

Fig. 4 shows the comparison of computed and experimental characteristics at corrected speed values $\bar{n} = 0.8$ and 1.0 with straight stator vanes and two rotor versions: with straight and sickle-like blades. Fig. 6 shows Mach number distribution in blade channels for the rotor and the stator as well distributions of total pressure ratio and adiabatic efficiency along the channel height at the stage outlet at optimum point of the characteristic $n = 1.0$.

While experimental values of the Stage parameters with two rotor versions (straight and sickle blades) show a noticeable difference in adiabatic efficiency, pressure ratio and max. air flow, this difference is hardly appreciable by calculations. At the same time, calculations are in good agreement with tests for straight rotor blades. As above-mentioned, in opinion of authors [3] et al. a probable cause of this difference is a change in conditions of unsteady interaction of rotor and stator rows in relative motion owing to displacement of phase interaction of elementary stages cascades located on different axisymmetrical streamline surfaces along the height. Other less probable reasoning lies in the fact that changes in intensity of secondary flows arising in case of replacement of a radial blade by a swept blade were not taken into account in calculations. Numerical and experimental investigations are under way in the direction of experimental data verification and mathematical model improvement.

Conclusions

1. Numerical and experimental investigations were completed for a high-loaded stage being a model of a typical HPC middle stage for an advanced turbofan with the

following design parameters: $U_{tip\ cor}=327$ m/s, $\bar{C}_{1a}=0.516$, $\bar{H}_T=0.404$, $\pi^*_{stage}=1.52$, $\eta^*_{ad}=0.88$.

2. The effects of bending in circumferential direction of longitudinal axes of stator vanes and rotor vanes were analyzed and applicability of rotor blades with a bent longitudinal axis for stages with increased aerodynamic loading in non-multistage high-loaded HPC of advanced turbofan were studied.

3. Among studied stage versions distinguished by various combinations of bent rotor blades and stator vanes, sickle rotor blades (with a concave pressure side surface) and straight stator vanes were chosen as the optimum version.

4. A considerable increase in adiabatic efficiency was experimentally measured for the optimum version $\Delta\eta^*_{ad} \sim 1.7 \div 2.0\%$ at rotational speeds $\bar{n}_{cor.}=0.8 \div 0.9$ of the nominal value and $\Delta\eta^*_{ad} \sim 0.7\%$ at $\bar{n}_{cor.}=1.0$. Moreover, there is an increase in airflow and pressure ratio.

5. Calculated values were compared with test results in operating conditions at rotational speeds $\bar{n}_{cor.}=0.8, 1.0$. Calculations were in good agreement with tests for straight rotor blades. By present time a considerable improvement of performances for the stage version with sickle rotor blades was not found by calculations as it was measured in experiment.

References

- [1] I.A. Brailko, V.I. Mileshin, M.A. Nyukhtikov, S.V. Pankov. "Computational And Experimental Investigation Of Unsteady And Acoustic Characteristics Of Counter – Rotating Fans". HT-FED-2004-56436, July 11-15, 2004, Charlotte, North Carolina, USA.
- [2] F.Sh. Gelmedov, N.M. Savin, Eu.I. Stepanov, L.I. Semernyak. Development of D-66 typical middle stage of low stage HPC with rotor blades spatial profiling. CIAM 2001-2005. Main results of science and research activity. Vol. 1. Edited by V.A. Skibin, V.I. Solonin, M.Ya. Ivanov. – M.:CIAM, 2005, - 472p.
- [3] I.A. Brailko, V.I. Mileshin, M.A. Nyukhtikov, S.V. Pankov, A.A. Rossikhin. "3D Computational Analysis of Unsteady and Acoustic Characteristics of a Model of High Bypass Ratio Counter-Rotating Fan". ISABE-2005-1186, September, 4-9, Munich, Germany.
- [4] V.E. Saren, N.M. Savin, et al. Hydrodynamic interaction of axial turbomachine cascades; Journal of Engineering Mathematics, Vol. 55, №1-4, (2006), 9-39.
- [5] V.I. Mileshin, I.K. Orekhov, S.V. Pankov "Numerical And Experimental Investigations Of Bypass Fans Characteristics" Proceedings of ISABE International Conference, Beijing, ISABE-2007-1179, 2007.
- [6] V.I. Mileshin, M.A. Nyukhtikov, I.K. Orekhov, S.V. Pankov, S.K. Shchipin "Open Counter – Rotation Fan Blades Optimization Based On 3d Inverse Problem Navier-Stokes Solution Method With The Aim Of Tonal Noise Reduction" Proceedings of GT2008 ASME Turbo Expo 2008, June 9-13, 2008, Berlin, Germany, GT2008-51173.

Contact Author Email Address

mileshin@ciam.ru

Copyright Statement

The authors confirm that they, and/or their company or organization, hold copyright on all of the original material included in this paper. The authors also confirm that they have obtained permission, from the copyright holder of any third party material included in this paper, to publish it as part of their paper. The authors confirm that they give permission, or have obtained permission from the copyright holder of this paper, for the publication and distribution of this paper as part of the ICAS2010 proceedings or as individual off-prints from the proceedings.

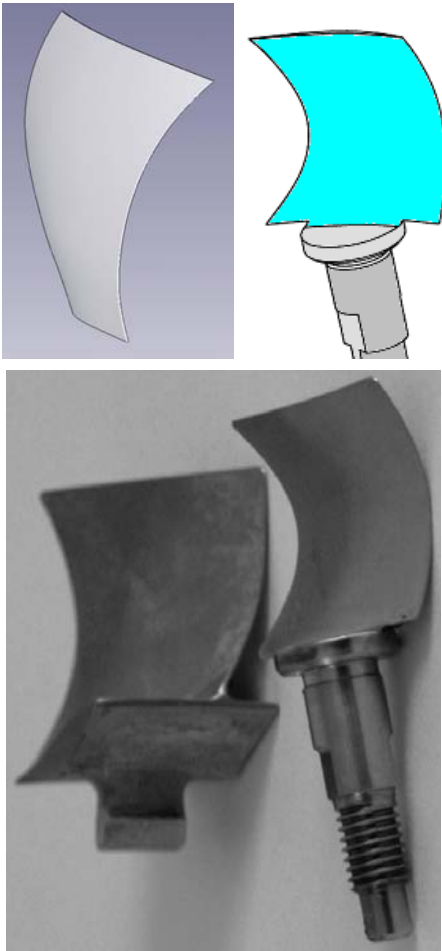


Fig. 2. Stator and rotor blades with curvilinear longitudinal axis
Sickle-like rotor and sabre-like stator

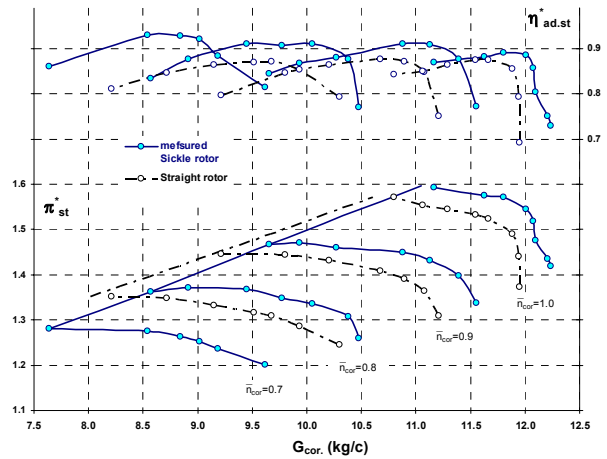


Fig. 3. Effects of rotor blade longitudinal axis shape on the Stage performances

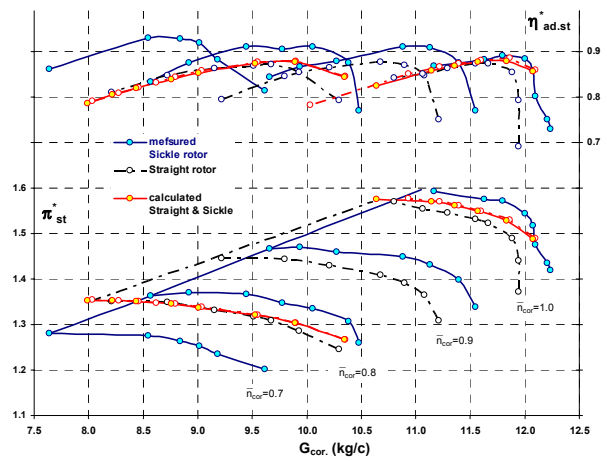


Fig. 4. Comparison of experimental and calculated data

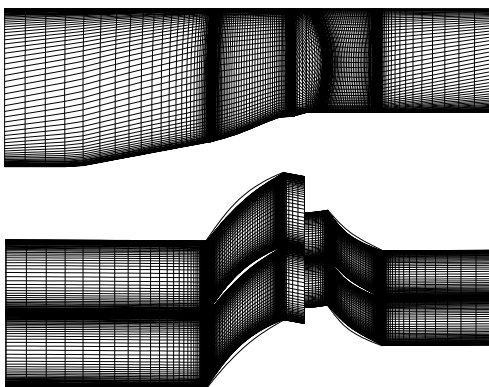


Fig. 5. Computational grids

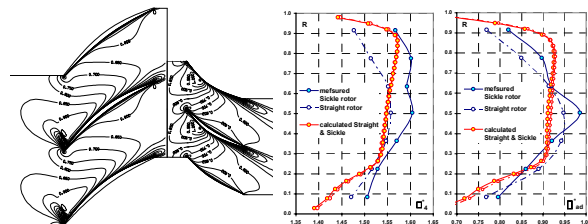


Fig. 6. Calculations of viscous 3D flows.
Mach number isolines, step= 0.05. Distribution of total pressure ratio and adiabatic efficiency along the channel height at the Stage outlet